ON PARTIAL STABILITY OF PREEMPTIVE PRIORITY RETRIAL MODEL

Ruslana Nekrasova

•

Institute of Applied Mathematical Research Karelian Research Centre, RAS,
Petrozavodsk State University, Russia
ruslana.nekrasova@mail.ru

Abstract

We consider a retrial model under constant retrial rate policy with two classes of customers characterized by different priorities. Preemptive priority arrivals, who meet the server busy by the other class customer, immediately start the processing, while interrupted customers lose the residual service times and join the end of the corresponding orbit queue. The system is fed by a superposition of two Poisson inputs, retrial times are exponential, service times are generally distributed and independent and iid in each class. We study the model in a partial stable state, when one orbit queue (independently of its class priority) is stochastically bounded, and other orbit infinitely grows in probability. We rely in preliminary results for a convenient two-class retrial model with no interruptions, where partial stability is equivalent to the transience of an associated Markov Chain (MC). Based on MC approach, we obtain transience conditions for embedded two-dimensional orbit size process and then verify partial stability behavior in transient zones by simulation.

Keywords: retrial model, constant retrial rate, preemptive priority, partial stability

1. Introduction

The paper deals with a single server two-class retrial model under constant retrial rate policy. Multi-class retrial systems have a wide sphere of applicability. For instance, such models can be successfully used in description of call centers [1, 2] or modern computer networks and protocols [3, 4]. Various types of retrial models are well presented in a corresponding literature. In this regard it is worth mention [5, 6, 7]. In particular [8, 9, 10] are dedicated to priority retrial queues.

We consider retrial system with two non-equivalent classes, characterized by different priorities. If the high (preemptive) priority arrival meets the server busy by the low priority customer, the service interruption occurs. In such a moment the low priority customer joins the corresponding orbit queue, while the high priority one starts processing. The system is fed by a superposition of two Poisson inputs, service times are generally distributed and independent and identically distributed (iid) in each class. The system contains two orbits under constant retrial rate policy, orbit attempts are exponential and retrial rates are defined by the corresponding class. Stability conditions for such a model have been obtained in a recent paper [11], where authors used an embedded MC approach. Previously such a method was successfully applied to the stability analysis of a two-class retrial model [12] and also to a retrial model with unreliable server [13]. The main purpose of the present paper is to study the so-called partially stable state, which arises when one orbit is stochastically bounded and other orbit infinitely grows in probability. In such a case the model is not totally stable, but we are able to use steady-state techniques to analyze the stable orbit. Note that in [14] regenerative method of confidence estimation was applied to a partially stable retrial model with two equivalent priority classes.

Partial stability conditions have been obtained in [12] for a conventional two-class retrial model. Based on the MC approach, the authors in [12] had shown that partial stability regimes are equivalent to the transient states of a two-dimensional MC associated with the orbit queue size components. Thus our goal is to obtain in an explicit form the transience conditions for the embedded MC in the model under consideration, then to verify partial stability behavior in transient mode by simulation.

The paper is organized as follows. Section 2 is devoted to the detailed description of the model. In Section 3 we present MC approach to stability analysis of two-class retrial model. Such a method allows to obtain the ergodicity/transience conditions of a MC associated with the orbit size components. Section 4 contains the new basic analytical result for transience conditions. In Section 5 we present simulation results for the model in transient and non-ergodic modes. The obtained results show that transient regimes correspond to the partial stability states. Section 6 concludes the paper.

2. Model Description

We construct two-class retrial model under constant retrial rate policy. The system is fed by a superposition of two Poisson inputs with corresponding rates λ_k, $k = 1, 2$. Define by τ_k generic interarrival time for the class-k customers. Note $\mathsf{E}\tau_k = 1/\lambda_k$, $k = 1, 2$.

If class-k new arrival is unable to receive service because of busy server, it joins to the corresponding infinite capacity orbit. Constant retrial rate policy implies that the orbit customers obey to FIFO discipline: the first in the orbit queue customer makes retrial attempts to capture the server. The retrial times are exponentially distributed and class-dependent. Define class-k retrial rate by σ_k.

Note that the model has non-equivalent classes. The first class of customers has so-called preemptive or high priority. Namely if the high priority arrival meets the other class customer on service, it captures the server immediately, while the low priority costumer joins the corresponding (class-2) orbit queue and an interruption occurs. Note that in case of successful retrial attempt an interrupted customer gets new independent service time, while its previous residual service time is lost. From this point of view the model under consideration has no work-conserving property. The low priority arrivals and the high priority arrivals who meet the server busy by the same class customer obey to the constant retrial rate policy. Note that class-1 retrials (orbit customers) loss its priority and are unable to interrupt the second class service.

Moreover we consider general and iid class-dependent service times. As the model is not Markovian. Stability analysis becomes much more complicated. Let S_k define class-k generic service time with the corresponding distribution function (d.f.) F_k. Thus

$$\mathsf{p}_0 := (S_2 \leq \tau_1) = \int_0^\infty e^{-\lambda_1 x} dF_2(x) \tag{1}$$

is the probability that the second class customer completed its service with no interruption. Note that p_0 is the Laplace-Stieltjes transform of the service time S_2. Let define class-k load coefficient $\rho_k = \lambda_k \mathsf{E} S_k$, $k = 1, 2$.

Next we define by $Y^{(k)}(t)$, $k = 1, 2$, and by $N(t) \in \{0, 1\}$, class-k orbit queue size and the number of customers on the server at instant $t \geq 0$, respectively. Now we construct a basic three-dimensional process

$$\mathbf{X} = \Big(Y^{(1)}(t),\, Y^{(2)}(t),\, N(t),\, t \geq 0\Big), \tag{2}$$

describing the dynamics of the system.

In this paper we are interested in so-called partial stability, which actually means that one orbit is tight, while other orbit infinitely grows in probability. Note the process $Y^{(k)}(t)$ is called tight [15], if for any finite constant $C \geq 0$ exists $\delta > 0$

$$\inf_t \mathsf{P}\big(Y^{(k)}(t) \leq C\big) \geq 1 - \delta.$$

3. Markov chain approach

Stability analysis based on the properties of the process $\mathbf{X}$ seems rather intuitive while the search of partial stability conditions is a challenging problem. To solve this problem, we use a method associated with the embedded MC. In this regard we consider two-dimension discrete time process

$$\mathbf{Y} = \Big(Y_n^{(1)},\, Y_n^{(2)}, \quad n \geq 1\Big), \tag{3}$$

where $Y_n^{(k)}$ defines the number of customers at class-k orbit just after the n-th departure instant (after service competition). As input stream is Poisson and retrial times are exponentially distributed, it is easy to show that the process $\mathbf{Y}$ is a homogeneous irreducible aperiodic MC.

It has been shown in paper [12] that, for a convenient two-class retrial system, stability of a basic process $\mathbf{X}$ is equivalent to the ergodicity of embedded MC $\mathbf{Y}$. Our goal is to extend the results from [12] for preemptive priority model. Note that in further analysis we define stability as ergodicity of MC $\mathbf{Y}$.

The method developed in [16] allows to obtain ergodicity and transience conditions for two-dimensional MC. Such an approach actually represents two-dimensional analogue of the negative drift condition. Namely, from Theorem 3.3.1 , [16] ergodicity and transience conditions for two-dimensional MC $\mathbf{Y}_n$ are expressed via appropriate combinations of the following four conditions or their opposites.

1. The first orbit negative drift condition:

$$\mathsf{E}\Big[Y_{n+1}^{(1)} - Y_n^{(1)}\Big| Y_n^{(1)} > 0, Y_n^{(2)} > 0\Big] < 0. \tag{4}$$

2. The second orbit negative drift condition:

$$\mathsf{E}\Big[Y_{n+1}^{(2)} - Y_n^{(2)}\Big| Y_n^{(1)} > 0, Y_n^{(2)} > 0\Big] < 0. \tag{5}$$

3. The first "joint" condition:

$$\begin{aligned}\mathsf{E}\Big[Y_{n+1}^{(1)} - Y_n^{(1)}\Big| Y_n^{(1)} = 0, Y_n^{(2)} > 0\Big]\mathsf{E}\Big[Y_{n+1}^{(2)} - Y_n^{(2)}\Big| Y_n^{(1)} > 0, Y_n^{(2)} > 0\Big] - \\ \mathsf{E}\Big[Y_{n+1}^{(1)} - Y_n^{(1)}\Big| Y_n^{(1)} > 0, Y_n^{(2)} > 0\Big]\mathsf{E}\Big[Y_{n+1}^{(2)} - Y_n^{(2)}\Big| Y_n^{(1)} = 0, Y_n^{(2)} > 0\Big] \quad \geq \quad 0.\end{aligned} \tag{6}$$

4. The second "joint" condition:

$$\begin{aligned}\mathsf{E}\Big[Y_{n+1}^{(1)} - Y_n^{(1)}\Big| Y_n^{(1)} > 0, Y_n^{(2)} > 0\Big]\mathsf{E}\Big[Y_{n+1}^{(2)} - Y_n^{(2)}\Big| Y_n^{(1)} > 0, Y_n^{(2)} = 0\Big] - \\ \mathsf{E}\Big[Y_{n+1}^{(1)} - Y_n^{(1)}\Big| Y_n^{(1)} > 0, Y_n^{(2)} = 0\Big]\mathsf{E}\Big[Y_{n+1}^{(2)} - Y_n^{(2)}\Big| Y_n^{(1)} > 0, Y_n^{(2)} = 0\Big] \quad \geq \quad 0.\end{aligned} \tag{7}$$

Note that in [11] by MC method were obtained stability conditions for a model under consideration. Authors in [12] applied MC approach for analysis of a retrial model with no interruptions and showed that transience state of two-dimensional MC associated with orbit queue components corresponds to partial stability regime. It is worth mention that results from [16] are applicable under some extra conditions, which automatically hold for the models with Poisson input, see Appendix A in [12] for details.

4. Transience conditions

One of our main goals in this paper is to obtain transience conditions for MC **Y** and then to verify partial stability behavior by simulation in transient mode. Theorem 3.3.1 from [16] defines two transience cases. Relying on [16] we consider transience - I, if

- the first orbit negative drift condition (4) holds;
- the second orbit negative drift condition (5) is violated;
- the first joint condition (6) holds true.

Symmetrically we define transience - II, if

- the first orbit negative drift condition (4) is violated;
- the second orbit negative drift condition (5) holds;
- the second joint condition (7) holds true.

Taking into account the results from [12], we can expect that transience - I mode corresponds to the first class partial stability (the first orbit is tight, the second orbit infinitely grows), while transience - II mode corresponds to the second class partial stability.

To obtain transience conditions in an explicit form we first deduce expressions for the mentioned above conditional mean drifts.

4.1. Mean drifts

We start from analysis of the expression

$$\mathsf{E}\Big[Y^{(1)}_{n+1}-Y^{(1)}_n\Big|Y^{(1)}_n>0,Y^{(2)}_n>0\Big],$$

which represents the first orbit mean drift on one step of MC under the condition that in the previous step both orbits were not empty.

Recall that input stream is Poisson and consider the probability that $j\geq 0$ customers join the class-k orbit on a random time interval distributed as S_i as follows:

$$p_k^{S_i}(j):=\int_{x=0}^{\infty}e^{-\lambda_k x}\frac{(\lambda_k x)^j}{j!}dF_i(x),\quad k=1,2;\ i=1,2;\ j\geq 0. \tag{8}$$

Next we analyze the first orbit mean increment for the one step of MC **Y** under the condition that on previous step both orbits were not empty. In case the first class customer is on service, j customers join the orbit with probability (w.p.) $p_1^{S_1}(j)$. From the other hand, if the second class customer is on service, the interruption may occur w. p. $(1-\mathsf{p}_0)$. In this case the arrival immediately starts its service and does not affect the orbit, while the further first class arrivals saturate the orbit on time interval distributed as S_1. In case of no interruption which arise w. p. $\mathsf{p}_0=\mathsf{P}(S_2\leq\tau_1)$ the first orbit drift is equal to zero (the low priority customer finishes its service before the high priority arrival joins the system). Thus

$$\mathsf{E}\Big[Y^{(1)}_{n+1}-Y^{(1)}_n\Big|Y^{(1)}_n>0,Y^{(2)}_n>0\Big]=\frac{\lambda_1}{\lambda_1+\sigma_1+\lambda_2+\sigma_2}\sum_{j=0}^{\infty}jp_1^{S_1}(j)$$
$$+\frac{\sigma_1}{\lambda_1+\sigma_1+\lambda_2+\sigma_2}\sum_{j=0}^{\infty}(j-1)p_1^{S_1}(j)+\big(1-\mathsf{p}_0\big)\frac{\lambda_2+\sigma_2}{\lambda_1+\sigma_1+\lambda_2+\sigma_2}\sum_{j=0}^{\infty}jp_1^{S_1}(j).$$

After some computation efforts (see [11] for details) we obtain

$$\mathsf{E}\Big[Y^{(1)}_{n+1}-Y^{(1)}_n\Big|Y^{(1)}_n>0,Y^{(2)}_n>0\Big]=\frac{\lambda_1\rho_1-\sigma_1(1-\rho_1)+(\sigma_2+\lambda_2)\big(1-\mathsf{p}_0\big)\rho_1}{\lambda_1+\sigma_1+\lambda_2+\sigma_2}. \tag{9}$$

Next we discuss the second orbit mean drift under condition that both orbits are not empty. If the first class customer is on service (or if no interruption occurs), class-2 customers join the corresponding orbit on interval distributed as S_1 (or S_2). In case of interruption, arrivals join the orbit on interval distributed as $\tau_1 + S_1$. Namely if the second class customer occupies the server and interruption occurs, w.p. $(1 - \mathsf{p}_0)$ the second class mean orbit drift is defined by

$$\frac{\lambda_2}{\lambda_1+\sigma_1+\lambda_2+\sigma_2}\sum_{j=0}^{\infty}(j+1)\sum_{k=0}^{j}p_2^{\tau_1}(k)p_2^{S_1}(j-k)+\frac{\sigma_2}{\lambda_1+\sigma_1+\lambda_2+\sigma_2}\sum_{j=0}^{\infty}j\sum_{k=0}^{j}p_2^{\tau_1}(k)p_2^{S_1}(j-k)\Big).$$

The total expression has the following view

$$\mathsf{E}\Big[Y_{n+1}^{(2)}-Y_n^{(2)}\Big|Y_n^{(1)}>0,Y_n^{(2)}>0\Big]=\Bigg[(\lambda_1+\sigma_1)\lambda_2\mathsf{E}S_1+\mathsf{p}_0\Big(\lambda_2\rho_2-\sigma_2(1-\rho_2)\Big)$$

$$+(1-\mathsf{p}_0)\lambda_2\Big(\lambda_2\mathsf{E}S_1+\frac{\lambda_2}{\lambda_1}+\lambda_2+\sigma_2\mathsf{E}S_1+\frac{\sigma_2}{\lambda_1}\Big)\Bigg]\Big/(\lambda_1+\sigma_1+\lambda_2+\sigma_2). \quad (10)$$

Joint conditions (6) and (7) contain mean orbit drifts for the cases when one of the orbits is empty on previous step. We can easily obtain such expressions from (9) and (10), setting $\sigma_1 = 0$ ($\sigma_2 = 0$), if $Y_k^{(1)} = 0$, $Y_k^{(2)} > 0$ ($Y_k^{(1)} > 0$, $Y_k^{(2)} = 0$).

4.2. Transience zones

To simplify further calculations we define some auxiliary values

$$\frac{1}{A_1} = (1-\mathsf{p}_0)\frac{\rho_1}{1-\rho_1}, \quad (11)$$

$$B_1 = \big(\lambda_1+\lambda_2(1-\mathsf{p}_0)\big)\frac{\rho_1}{1-\rho_1}, \quad (12)$$

$$\frac{1}{A_2} = \big(-\mathsf{p}_0(1-\rho_2)+(1-\mathsf{p}_0)(\lambda_2\mathsf{E}S_1+\frac{\lambda_2}{\lambda_1})\big)/\lambda_2\mathsf{E}S_1, \quad (13)$$

$$B_2 = \big(\rho_1+\mathsf{p}_0\rho_2+(1-\mathsf{p}_0)(\lambda_2\mathsf{E}S_1+\frac{\lambda_2}{\lambda_1}+1)\big)/\mathsf{E}S_1. \quad (14)$$

Note that $B_2 > 0$, the sign of A_2 may vary and for $\rho_1 < 1$ we have A_1, $B_1 > 0$. Thus we obtain

$$\mathsf{E}\Big[Y_{n+1}^{(1)}-Y_n^{(1)}\Big|Y_n^{(1)}>0,Y_n^{(2)}>0\Big] = \frac{1-\rho_1}{\lambda_1+\sigma_1+\lambda_2+\sigma_2}\big(-\sigma_1+\frac{1}{A_1}\sigma_2+B_1\big), \quad (15)$$

$$\mathsf{E}\Big[Y_{n+1}^{(2)}-Y_n^{(2)}\Big|Y_n^{(1)}>0,Y_n^{(2)}>0\Big] = \frac{\lambda_2\mathsf{E}S_1}{\lambda_1+\sigma_1+\lambda_2+\sigma_2}\big(\sigma_1+\frac{1}{A_2}\sigma_2+B_2\big) \quad (16)$$

and then formulate joint conditions (6) and (7) as follows.
The first joint condition:

$$(1-\rho_1)\Bigg(\Big(\frac{1}{A_1}\sigma_2+B_1\Big)\Big(\sigma_1+\frac{1}{A_2}\sigma_2+B_2\Big)-\Big(-\sigma_1+\frac{1}{A_1}\sigma_2+B_1\Big)\Big(\frac{1}{A_2}\sigma_2+B_2\Big)\Bigg) \geq 0$$

$$(1-\rho_1)\Bigg(\sigma_2\Big(\frac{1}{A_1}+\frac{1}{A_2}\Big)+B_1+B_2\Bigg) \geq 0. \quad (17)$$

The second joint condition:

$$\frac{(1-\rho_1)}{A_1A_2}\Bigg(\sigma_1\Big(A_1+A_2\Big)+B_2A_2-B_1A_1\Bigg) \geq 0. \quad (18)$$

Next we present the basic analytical result.

Theorem 1. Consider two-class retrial model with constant retrial rate and preemptive priority of the first class customers.

1. If $\rho_1 < 1$, then the first orbit negative drift condition

$$\lambda_1\rho_1 - \sigma_1(1-\rho_1) + (\sigma_2+\lambda_2)(1-\mathsf{p}_0)\rho_1 < 0$$

defines transience-I regime, if one of the following alternative cases holds true

a).

$$\begin{cases}\lambda_2(1-\mathsf{p}_0) < \lambda_1\mathsf{p}_0(1-\rho_1)(1-\rho_2)\\ \sigma_2 \le \lambda_2\frac{\mathsf{p}_0\lambda_1\left(1-(1-\rho_1)(1-\rho_2)\right)+(\lambda_1+\lambda_2)(1-\mathsf{p}_0)}{\lambda_1\mathsf{p}_0\left(1-(1-\rho_1)(1-\rho_2)\right)-\lambda_2(1-\mathsf{p}_0)}\end{cases}; \tag{19}$$

b).

$$\lambda_1\mathsf{p}_0(1-\rho_1)(1-\rho_2) \le \lambda_2(1-\mathsf{p}_0) < \lambda_1\mathsf{p}_0(1-\rho_2) - \lambda_2(1-\mathsf{p}_0)\rho_1; \tag{20}$$

c).

$$\lambda_2(1-\mathsf{p}_0)(\rho_1+1) \ge \lambda_1\mathsf{p}_0(1-\rho_2). \tag{21}$$

2. If $\lambda_2(1-\mathsf{p}_0)(\rho_1+1) < \lambda_1\mathsf{p}_0(1-\rho_2)$, then the second orbit negative drift condition

$$(\lambda_1+\sigma_1)\lambda_2\mathsf{E}S_1 + \mathsf{p}_0\Big(\lambda_2\rho_2 - \sigma_2(1-\rho_2)\Big) + (1-\mathsf{p}_0)\lambda_2\Big(\lambda_2\mathsf{E}S_1 + \frac{\lambda_2}{\lambda_1} + \lambda_2 + \sigma_2\mathsf{E}S_1 + \frac{\sigma_2}{\lambda_1}\Big) < 0$$

defines transience-II regime, if one of the following alternative cases holds true

a).

$$\begin{cases}\lambda_2(1-\mathsf{p}_0) < \lambda_1\mathsf{p}_0(1-\rho_1)(1-\rho_2)\\ \sigma_1 \le \lambda_1\frac{\lambda_1\mathsf{p}_0\rho_1(1-\rho_2)}{\lambda_1\mathsf{p}_0(1-\rho_1)(1-\rho_2)-\lambda_2(1-\mathsf{p}_0)}\end{cases}; \tag{22}$$

b).

$$\begin{cases}\rho_1 < 1\\ \lambda_2(1-\mathsf{p}_0) \ge \lambda_1\mathsf{p}_0(1-\rho_1)(1-\rho_2)\end{cases}; \tag{23}$$

c).

$$\rho_1 \ge 1. \tag{24}$$

Proof. First our goal is to analyze the sets of transience conditions from [16] for various signs of parameters A_k, B_k. Let discuss all the possible cases separately.

Case 1: $\rho_1 < 1$.

The current case automatically implies A_1, $B_1 > 0$, see (11), (12). The first orbit negative drift condition is obtained as follows

$$\sigma_2 < A_1\sigma_1 - A_1B_1 =: f_1(\sigma_1), \tag{25}$$

where f_1 is a linear increasing function with an argument σ_1 and coefficients defined via λ_k, $\mathsf{E}S_k$, $k = 1, 2$ and p_0. Next we analyze various signs of A_2.

Case 1.1: $\rho_1 < 1$, $A_2 < 0$.

Now we express the second orbit negative drift condition as

$$\sigma_2 > -A_2\sigma_1 - A_2B_2 =: f_2(\sigma_1), \tag{26}$$

where f_2 is a linear increasing function.

Note that condition $A_2 < 0$ or equivalently $1/A_2 < 0$ is presented as

$$\lambda_2(1-\mathsf{p}_0)(\rho_1+1) < \lambda_1\mathsf{p}_0(1-\rho_2). \tag{27}$$

Case 1.1.1: $\rho_1 < 1$, $A_2 < 0$, $A_1 + A_2 > 0$.
We define the first and the second joint conditions respectively as

$$\sigma_2 \leq -A_1 A_2 \frac{(B_1 + B_2)}{A_1 + A_2} := \sigma_2^*, \tag{28}$$

$$\sigma_1 \leq \frac{A_1 B_1 - A_2 B_2}{A_1 + A_2} := \sigma_1^*. \tag{29}$$

Note that in this case $\sigma_1^*, \sigma_2^* > 0$. Moreover for any arbitrary signs of A_k, B_k we can show that $f_1(\sigma_1^*) = f_2(\sigma_1^*) = \sigma_2^*$, see [11] for detailed calculations. Transience-I zone in the current case corresponds to the following set of conditions:

$$\sigma_2 < f_1(\sigma_1),\ \sigma_2 \leq f_2(\sigma_1),\ \sigma_2 \leq \sigma_2^*,$$

while transience-II is defined by:

$$\sigma_2 \geq f_1(\sigma_1),\ \sigma_2 > f_2(\sigma_1),\ \sigma_1 \leq \sigma_1^*.$$

The relation $A_1 > -A_2$ implies $f_1(\sigma_1) > f_2(\sigma_1)$ for $\sigma_1 > \sigma_1^*$, $\sigma_2 > \sigma_2^*$. Transience zones for the particular case of uniform service times distributed on corresponding intervals $[a_k, b_k]$, $k = 1, 2$ (define $S_k \sim \mathsf{U}[a_k, b_k]$) are presented on Fig 1, the left picture. Namely we set

$$\lambda_1 = 1.5,\ \lambda_2 = 0.8,\ S_1 \sim U[0.1, 0.7],\ S_2 \sim U[0.05, 0.45] \tag{30}$$

and obtain

$$\mathsf{p}_0 \approx 0.6976,\ A_1 = 2.2,\ A_2 = -1.1,\ B_1 = 2.6,\ B_2 = 3.2,\ \sigma_1^* = 8.1,\ \sigma_2^* = 12.1. \tag{31}$$

Note that in [11] was obtained that under conditions $\rho_1 < 1$, $A_2 < 0$, $A_1 + A_2 > 0$ the zone $\sigma_1 > \sigma_1^*$, $\sigma_2 > \sigma_2^*$ defines stability region for the model under consideration.

Case 1.1.1: $\rho_1 < 1$, $A_2 < 0$, $A_1 + A_2 > 0$.   Case 1.1.2: $\rho_1 < 1$, $A_2 < 0$, $A_1 + A_2 < 0$.

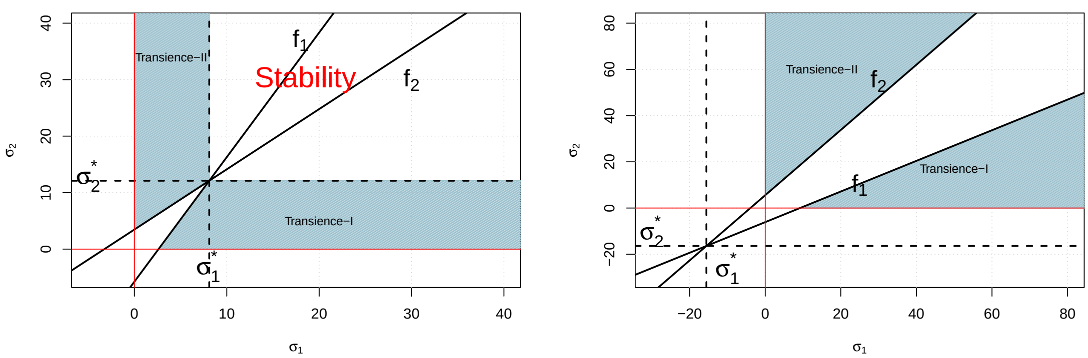

Figure 1: *Transience zones.*

Moreover the left picture from Figure 1 illustrates that in both transience modes non-negative drift conditions are redundant.

The condition $A_1 + A_2 > 0$ is equivalent to

$$\lambda_2 \mathsf{E} S_1 (1 - \mathsf{p}_0)\rho_1 < (1 - \rho_1)\Big(\mathsf{p}_0(1 - \rho_2) - (1 - \mathsf{p}_0)(\lambda_2 \mathsf{E} S_1 + \lambda_2/\lambda_1\Big)$$
$$\lambda_2(1 - \mathsf{p}_0) < \lambda_1 \mathsf{p}_0 (1 - \rho_1)(1 - \rho_2). \tag{32}$$

From (27) and (32) we have

$$\lambda_2(1 - \mathsf{p}_0) < \lambda_1 \mathsf{p}_0(1 - \rho_2) - \max\Big(\lambda_2(1 - \mathsf{p}_0), \lambda_1 \mathsf{p}_0(1 - \rho_2)\Big)\rho_1. \tag{33}$$

RT&A, Special Issue, No 8 (85)
Volume 20, July 2025

The relation $\lambda_2(1 - \mathsf{p}_0) \geq \lambda_1 \mathsf{p}_0 (1 - \rho_2)$ violates the condition (27). Thus (33) turns to

$$\lambda_2(1 - \mathsf{p}_0) < \lambda_1 \mathsf{p}_0 (1 - \rho_1)(1 - \rho_2). \tag{34}$$

Hence the pair of conditions $A_2 < 0$ and $A_1 + A_2 > 0$ is implied by (34).

Case 1.1.2: $\rho_1 < 1$, $A_2 < 0$, $A_1 + A_2 < 0$.

For this case both joint conditions change the signs and turn to $\sigma_k \geq \sigma_k^*$, while $f_2(\sigma_1)$ dominates $f_1(\sigma_1)$ for $\sigma_1 > \sigma_1^*$, $\sigma_2 > \sigma_2^*$. Moreover $\sigma_k < 0$, $k = 1, 2$, see expressions in (28), (29).

Transience-I corresponds to the set of conditions

$$\sigma_2 < f_1(\sigma_1),\ \sigma_2 \leq f_2(\sigma_1),\ \sigma_2 \geq \sigma_2^*,$$

and transience-II is defined by :

$$\sigma_2 \geq f_1(\sigma_1),\ \sigma_2 < f_2(\sigma_1),\ \sigma_1 \geq \sigma_1^*.$$

Transience zones presented on Figure 1 (the right picture) illustrate that k-type transience is totally defined by the corresponding negative drift condition. Note that for this case we set

$$\lambda_1 = 2,\ \lambda_2 = 0.8,\ S_1 \sim U[0.1, 0.7],\ S_2 \sim U[0.05, 0.45] \tag{35}$$

and obtain

$$\mathsf{p}_0 \approx 0.6228,\ A_1 = 0.7,\ A_2 = -1.4,\ B_1 = 8.7,\ B_2 = 4.0,\ \sigma_1^* = -15.6,\ \sigma_2^* = -16.4. \tag{36}$$

Case 1.1.3: $\rho_1 < 1$, $A_2 < 0$, $A_1 + A_2 = 0$.

In this case both joint conditions (17) and (18) hold true because the left hand sides do not depend on retrial rates and are strictly positive, moreover note that f_1 and f_2 are parallel linear functions. The relation

$$-A_1 B_1 < 0 < -A_2 B_2$$

implies $f_1(\sigma_1) < f_2(\sigma_1)$ for any σ_1. Thus similar to the the case 1.1.2. we can show that k-type transience is defined by the corresponding negative drift condition.

Next we analyze the condition $A_1 + A_2 \leq 0$ which corresponds to cases 1.1.2 and 1.1.3. Relying on (32) we obtain

$$\lambda_2(1 - \mathsf{p}_0)\rho_1 \geq \lambda_1 \mathsf{p}_0 (1 - \rho_2) - \lambda_1 \mathsf{p}_0 (1 - \rho_2). \tag{37}$$

Combining with (27) we have

$$\lambda_1 \mathsf{p}_0 (1 - \rho_2) - \lambda_1 \mathsf{p}_0 (1 - \rho_2)\rho_1 \leq \lambda_2(1 - \mathsf{p}_0) < \lambda_1 \mathsf{p}_0 (1 - \rho_2) - \lambda_2(1 - \mathsf{p}_0)\rho_1. \tag{38}$$

Note that by (27) $\lambda_1 \mathsf{p}_0 (1 - \rho_2)\rho_1 > \lambda_2(1 - \mathsf{p}_0)\rho_1$, thus the solution set for (38) is not empty. Recall that (38) is equivalent to $A_2 < 0$, $A_1 + A_2 \leq 0$.

Case 1.2: $\rho_1 < 1$, $A_2 > 0$.

The second orbit negative drift condition transforms to $\sigma_2 < f_2(\sigma_1)$, where f_2 is a linear decreasing function. The first joint condition transforms to $\sigma_2 \geq \sigma_2^*$, and always holds true, as $\sigma_2^* < 0$. The second joint condition transforms to $\sigma_1 \geq \sigma_1^*$, the sign of σ_1^* may vary. Transience-I is described by the conditions

$$\sigma_2 < f_1(\sigma_1),\ \sigma_2 \geq f_2(\sigma_1),\ \sigma_2 \geq \sigma_2^*,$$

while transience-II is defined by the following set

$$\sigma_2 \geq f_1(\sigma_1),\ \sigma_2 < f_2(\sigma_1),\ \sigma_1 \geq \sigma_1^*.$$

In the current case the condition $f_2(\sigma_1) > 0$ holds only for negative values of σ_1. Hence the second orbit negative drift condition is violated and transience-II zone is empty. From the other hand, transience-I is defined by the first orbit negative drift condition, see Figure 2, where

$$\lambda_1 = 2,\ \lambda_2 = 0.8,\ S_1 \sim U[0.1, 0.7],\ S_2 \sim U[0.05, 0.95] \tag{39}$$

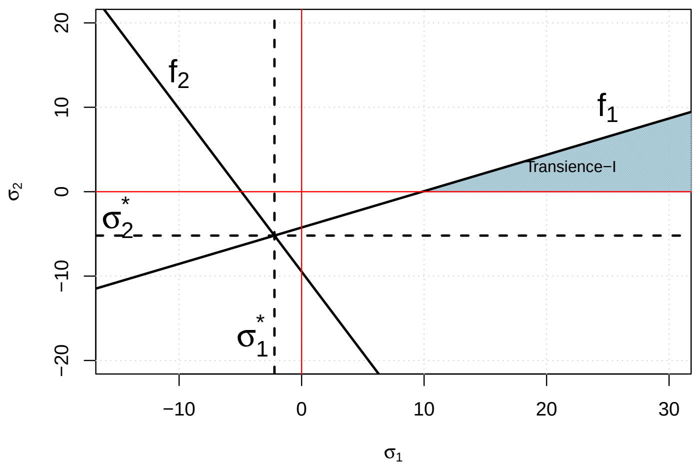

Figure 2: *Transience zones,* $\rho_1 < 1$, $A_2 > 0$.

and

$$p_0 \approx 0.4196,\ A_1 = 0.4,\ A_2 = 1.9,\ B_1 = 10.8,\ B_2 = 5.0,\ \sigma_1^* = -2.2,\ \sigma_2^* = -5.2. \tag{40}$$

Case 1.3: $\rho_1 < 1$, $1/A_2 = 0$.
The second orbit negative drift condition turns to $\sigma_1 + B_2 < 0$ and is violated. Thus transience-II zone is empty. Hence the second orbit non negative drift condition always holds true, moreover the first joint condition always holds true, see (17). Thus transience-I zone is defined by the first orbit negative drift condition.

Note that $1/A_2 \geq 0$ is equivalent to

$$\lambda_2(1 - p_0)(\rho_1 + 1) \geq \lambda_1 p_0 (1 - \rho_2). \tag{41}$$

Case 2: $\rho_1 > 1$.
This case automatically implies $A_1 < 0$, $B_1 < 0$. Thus after multiplying (15) by $A_1/(1-\rho_1) > 0$ we have the first orbit negative drift condition as $\sigma_2 < f_1(\sigma_1)$, where $f_1(\sigma_1) = A_1\sigma_1 - A_1B_1$ is a **decreasing** function. Moreover by definition we have $f_1 < 0$ for $\sigma_1 \geq 0$. Thus the first orbit negative drift condition is violated and transience-I zone is empty.

Case 2.1: $\rho_1 > 1$, $A_2 < 0$.
The second orbit negative drift condition is defined as $\sigma_2 > f_2(\sigma_1)$, where f_2 increases. The second joint condition evaluates to $\sigma_1 \geq \sigma_1^*$, while $\sigma_1^* < 0$. Thus negative drift condition defines transience mode for the second class orbit.

Case 2.2: $\rho_1 > 1$, $A_2 > 0$.
The second orbit negative drift condition is defined as $\sigma_2 < f_2(\sigma_1)$ and f_2 decreases. We have

$$f_2(\sigma_1) = -A_2\sigma_1 - A_2B_2.$$

Hence $f_2 < 0$ for $\sigma_1 \geq 0$, the second orbit negative drift condition is violated and transience-II zone is empty.

Case 2.3: $\rho_1 > 1$, $1/A_2 = 0$.
The second orbit negative drift condition turns to $\sigma_1 < -B_2$, thus transience-II zone is empty.

Case 3: $\rho_1 = 1$.
In this case $A_1 = 0$, while $B_1A_1 > 0$, see (11), (12). The second joint condition evaluates to

$$\sigma_1 \geq \frac{A_1B_1}{A_2} - B_2 \equiv \sigma_1^*. \tag{42}$$

If $A_2 < 0$ holds true, transience-II zone is defined by the second orbit negative drift condition. Next similar to the cases 2.2 and 2.3 we can show that for the case $1/A_2 \geq 0$ transience-II zone is empty.

Summing up, we group all the cases in Table 1.

Table 1: *Transience zones.*

	$\rho_1 < 1$			$\rho_1 \geq 1$	
	$1/A_2 < 0$		$1/A_2 \geq 0$	$1/A_2 < 0$	$1/A_2 \geq 0$
	$A_1 + A_2 > 0$	$A_1 + A_2 \leq 0$			
Transience-I	Neg. drift, $\sigma_2 \leq \sigma_2^*$.	Neg. drift.		-	
Transience-II	Neg. drift, $\sigma_1 \leq \sigma_1^*$.	Neg. drift.	-	Neg. drift.	-

Finally, relying on analysis from [11] we can show that

$$\sigma_1^* = \lambda_1 \frac{\lambda_1 \mathsf{p}_0 \rho_1 (1-\rho_2)}{\lambda_1 \mathsf{p}_0 (1-\rho_1)(1-\rho_2) - \lambda_2 (1-\mathsf{p}_0)}, \tag{43}$$

$$\sigma_2^* = \lambda_2 \frac{\mathsf{p}_0 \lambda_1 \big(1-(1-\rho_1)(1-\rho_2)\big) + (\lambda_1+\lambda_2)(1-\mathsf{p}_0)}{\lambda_1 \mathsf{p}_0 \big(1-(1-\rho_1)(1-\rho_2)\big) - \lambda_2(1-\mathsf{p}_0)}. \tag{44}$$

Hence basing on the results in table 1 and (43), (44), we prove the theorem. ■

Remark. Now we formulate a few comments to the presented Theorem.

1. Condition $\rho_1 < 1$ is a transience-I necessary condition. This demand is rather natural, as in this case we can expect the first orbit partial stability.
2. Condition $\lambda_1(1-\mathsf{p}_0)(\rho_1+1) < \lambda_1 \mathsf{p}_0 (1-\rho_2)$ or equivalently
$$(1-\mathsf{p}_0)\lambda_2 \mathsf{E}\big(S_1+\tau_1\big) < \mathsf{p}_0(1-\rho_2) \tag{45}$$
is a transience-II necessary condition. Note that $\mathsf{E}\big(S_1+\tau_1\big)$ defines a mean time from the moment when the second class "interrupted to be" customer captures the server up to the moment when the server becomes idle. Thus $\lambda_2\mathsf{E}\big(S_1+\tau_1\big)$ defines some kind of the probability that the server is busy in case of interruption: the second class customer is on service and then it is replaced by the preemptive priority arrival. From this point of view the left hand side of (45) defines the probability that interruption actually occurs. While the right hand side of (45) defines the probability that the interruption was not detected (the server is not occupied by the second class customer w.p. $(1-\rho_2)$). Note that (45) automatically implies a weaker necessary stability condition $\rho_2 < 1$.
3. From [11] we have that model is stable only if $\rho_1 < 1$, $A_2 < 0$, $A_1 + A_2 > 0$. In this case the pair of conditions $\sigma_1 < \sigma_1^*$, $\sigma_2 < \sigma_2^*$ is a stability criterion. Thus the second conditions in systems (19) and (22) provide instability for the the second and the first orbit, respectively.

5. Simulations

In this section we present simulation results in various cases from Theorem 1. Namely our goal is to show that the k-th type of transience mode defines the partial stability of the corresponding orbit.

We estimate mean orbit dynamics as follows. Consider $y_i^{(k)}(j)$ – the number of customers at k-class orbit just before the j-th arrival instant based on the i-th trajectory, $i = 1, \ldots, m$, $m = 100$. Namely we construct the following two-component sequence

$$\Big(\frac{1}{m}\sum_{i=1}^{m} y_i^{(1)}(j),\ \frac{1}{m}\sum_{i=1}^{m} y_i^{(2)}(j)\Big), \quad j = 1, \ldots n,\ n = 20\,000$$

and calculate the maximal values for the corresponding components

$$Max.Orb_k := \max_j \left(\frac{1}{m} \sum_{i=1}^{m} y_i^{(k)}(j) \right), \quad k = 1, 2.$$

In k-type transience mode we expect stable behavior of k-class orbit process and increasing of the other orbit process. Moreover a significant deviation of $Max.Orb_1$ and $Max.Orb_2$ also may indicate the partial stability of the orbit with the smaller maximal value.

Next we consider the model with uniform service time and star from the case 1.1.1 where $\rho_1 < 1$, $A_2 < 0$, $A_1 + A_2 > 0$. Input rates and mean service times coincide with the corresponding values (30). See table 2 for the explicit values for retrial rates used in simulation tests, test points (σ_1, σ_2) in transience and non-ergodic zones are presented on Figure 3, the left picture.

Case 1.1.1 Case 1.1.2

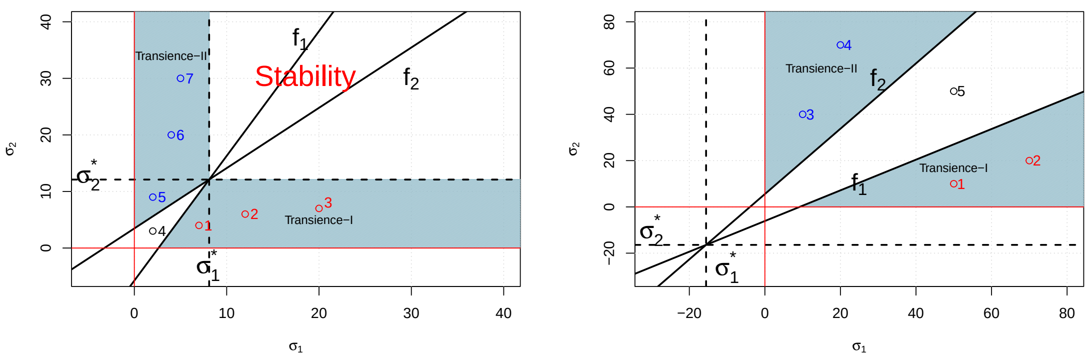

Figure 3: *Test points.*

Recall that in case 1.1.1 we have $\rho_1 = 0.6$, $A_1 = 2.1$, $A_2 = -1.1$. Tests 1–3 belong to transience-I zone, moreover moving from 1 to 3 we go closer to the stability border, and as a consequence the mean values for maximal orbit size decrease, see table 2. From the other hand, in these tests the maximal value of the first class orbit (Max. Orb_1) is not greater that 6.1, which may define the stable behavior, while the maximal value of the second class orbit (Max. Orb_2) strongly dominates Max. Orb_1. Such a phenomenon occurs in case of the first orbit partial stability. The results for transience-II zone (tests 5–7) are symmetrical, see table 2.

Orbit dynamics in transience modes (tests 2 and 6) are presented on Figure 4, the left picture. The grey lines correspond to the model in transience-I zone. The solid line illustrates the behavior of the first class orbit process. The dynamics is stable. From the other hand the dash line increases, thus we can expect that the mean value of the second class orbit size goes to infinity. Hence we observe the partly stable mode. The orbits behavior in transience-II zone also correspond to the assumption of partial stability. The black lines from the Figure 4 (the left picture) illustrate the test 6. The second class orbit (solid line) is stable, the first class orbit (dash line) infinitely grows.

The other interest is a model behavior in non-ergodic regime (test 4). See the mean orbits dynamics on Figure 4, the right picture, grey lines. Both orbits grow. Such a phenomenon corresponds to total instability and is predictable in non-ergodic zone. Note that the first class orbit process (solid line) strongly dominated the second class orbit process (dash line). Thus the first orbit is much more saturated. Such a result from the first site looks a bit confusing, as the first class customers have the high priority. The explanation is the following. Note that in the current example $\rho_1 = 0.6$, $\rho_2 = 0.2$, $\lambda_1 = 1.5$, $\lambda_2 = 0.8$ and $\sigma_1 = 2$, $\sigma_2 = 3$. Thus $\rho_1 > \rho_2$, hence the "load" from the first class is greater, the arrivals are more intensive. Moreover $\sigma_1 < \sigma_2$, consequently the second orbit is "faster". As a result we obtain the less number of the second class arrivals and more intensive attempts from the corresponding orbit, which lead to the smaller (in comparison with the other class) number of orbit customers.

Next we discuss the case 1.1.2 where $\rho_1 < 1$, $A_2 < 0$, $A_1 < -A_2$ and the basic parameters are defined in (35). Retrial rates are presented in table 2 and on Figure 3, the right picture. Tests 1–4 illustrate the orbits behavior in transience modes. The obtained results correspond to the assumption of partial stability and are additionally confirmed by the maximal values of mean orbit sizes, see table 2. The test 5 corresponds to non-ergodic zone, and we can expect the total instability. Note that obtained values $Max.Orb_1 = 1204$ and $Max.Orb_2 = 85$ are rather small in comparison with the other unstable cases. Thus to study such a test in details, we illustrate the mean orbit dynamics on Figure 4, the right picture, black lines. The first class orbit (dash line) strongly dominates the second class orbit (solid line). Note that $\rho_1 = 0.8$, $\rho_2 = 0.2$, $\lambda_1 = 2$, $\lambda_2 = 0.8$ and $\sigma_1 = 50$, $\sigma_2 = 50$. The first class arrivals are more intensive, which leads to the greater values of orbit size process. Note that the second class orbit process also grows. Thus the model is totally unstable.

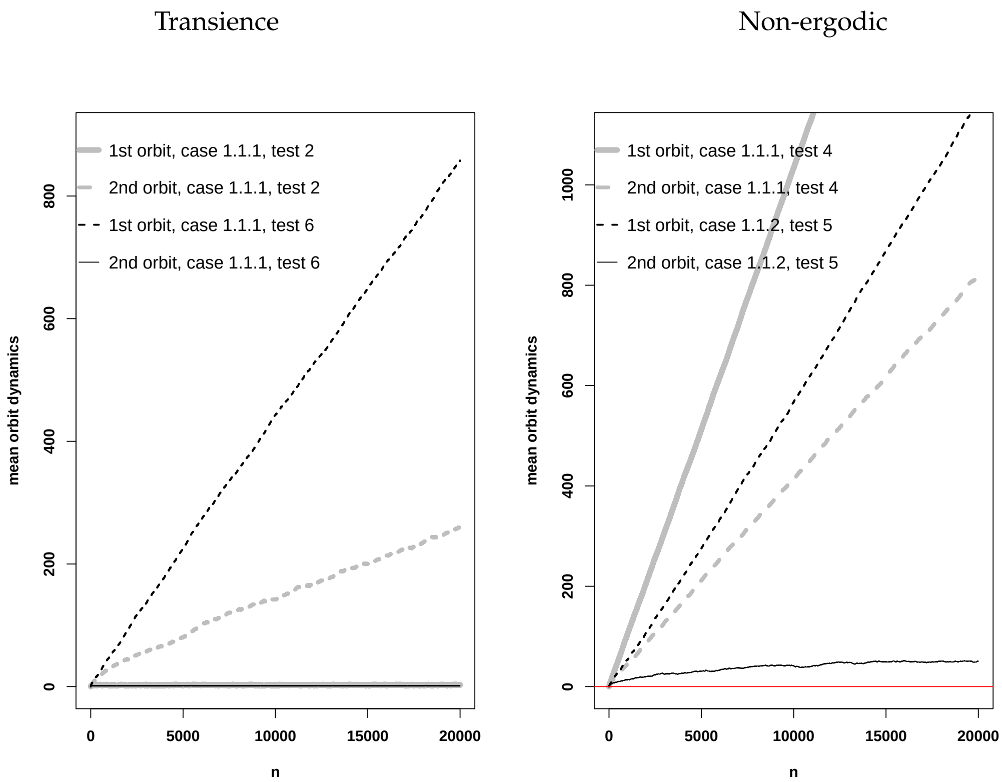

Figure 4: *Orbit dynamics.*

The results for the case 1.2, where $\rho_1 < 1, A_2 > 0$ and parameters are defined in (39), are presented in table 2. The assumption of partial stability is confirmed. Finally for the case 2.1, where $\rho_1 > 1, A_2 < 0$, we define

$$\lambda_1 = 1.5,\ \lambda_2 = 0.8,\ S_1 \sim U[0.5,\ 1.5],\ S_2 \sim U[0.05,\ 0.45]$$

and obtain

$$\mathsf{p}_0 \approx 0.6977,\ A_1 = -1.1,\ A_2 = -5.2,\ B_1 = -5.2,\ B_2 = 2.4, \sigma_1^* = -2.9,\ \sigma_2^* = -2.6.$$

The simulation results correspond with the assumption of patial stability. The model is totally unstable in non-ergodic zone.

Table 2: *Simulation results.*

Case	Test	σ_1	σ_2	Max. Orb_1	Max. Orb_2	Mode
1.1.1	1	7	4	6.1	319.9	Tr.-I
	2	12	6	3.8	260.8	Tr.-I
	3	20	7	2.6	65.1	Tr.-I
	4	2	3	2059.4	809.9	non-ergodic
	5	22	9	2284.2	2.8	Tr.-II
	6	4	20	857.9	2.1	Tr.-II
	7	5	30	369.9	1.9	Tr.-II
1.1.2	1	50	10	8.07	2591.2	Tr.-I
	2	70	20	9.54	1965.2	Tr.-I
	3	10	40	2596.3	2.7	Tr.-II
	4	20	70	1817.7	3.1	Tr.-II
	5	50	50	1204	89	non-ergodic
1.2	1	27	3	10.87	4652.5	Tr.-I
	2	12	6	9.54	1965.2	Tr.-I
	3	10	10	2705	2991	non-ergodic
2.1	1	7	60	6669	38	Tr.-II
	2	5	45	6921	20	Tr.-II
	3	20	45	6363	754	non-ergodic
	4	40	60	6106	2037	non-ergodic

6. Conclusion

The research is related to the phenomenon of partial stability in a two-class retrial model with preemptive priority of the first class customers and interruptions. Partially stable mode arises when queue size process in one of the orbits is stable, while in the other infinitely increases. Relying on MC approach we obtained transient conditions for MC, associated with orbit components at departure instants. Then basing on preliminary results for a convenient two-class retrial model with no interruptions, where transience defines partial stability, we verified by simulation partially stable state in transient zones. The simulation results had shown that under obtained transient conditions the model illustrates partially stable behavior.

Summing up, we can expect that transient zone implies the stability for one of the classes. Moreover relying on the assumption of partial stability in transient state, we can manage the model parameters to provide the service completion at finite time for the customers from the selected (even low priority) class, while the other (high priority) class customers sojourn time at corresponding orbit infinitely grows, and the whole model is unstable.

References

[1] Tuan Phung-Duc et al. "Retrial queues with balanced call blending: analysis of single-server and multiserver model". In: *Annals of Operations Research* 239.2 (Apr. 2014), pp. 429–449. ISSN: 1572-9338. DOI: 10.1007/s10479-014-1598-2.

[2] Evsey Morozov et al. "Performance analysis and stability of multiclass orbit queue with constant retrial rates and balking". In: *Performance Evaluation* 134 (Oct. 2019), p. 102005. ISSN: 0166-5316. DOI: 10.1016/j.peva.2019.102005.

[3] Konstantin Avrachenkov, Philippe Nain, and Uri Yechiali. "A retrial system with two input streams and two orbit queues". In: *Queueing Systems* 77.1 (Aug. 2013), pp. 1–31. ISSN: 1572-9443. DOI: 10.1007/s11134-013-9372-8.

[4] Evsey Morozov and Tuan Phung-Duc. "Regenerative Analysis of Two-Way Communication Orbit-Queue with General Service Time". In: *Queueing Theory and Network Applications*. Springer International Publishing, 2018, pp. 22–32. ISBN: 9783319937366. DOI: 10.1007/978-3-319-93736-6_2.

[5] J. Falin and James G. C. Templeton. *Retrial Queues*. en. London: Chapman and Hall/CRC, 1997.

[6] Jesús R. Artalejo and Antonio Gómez-Corral. *Retrial Queueing Systems*. Springer Berlin Heidelberg, 2008. ISBN: 9783540787259. DOI: 10.1007/978-3-540-78725-9.

[7] Tuan Phung-Duc. *Retrial Queueing Models: A Survey on Theory and Applications*. 2019. DOI: 10.48550/ARXIV.1906.09560.

[8] Yi Peng. "On the discrete-time Geo/G/1 retrial queueing system with preemptive resume and Bernoulli feedback". In: *OPSEARCH* 53.1 (July 2015), pp. 116–130. ISSN: 0975-0320. DOI: 10.1007/s12597-015-0218-5.

[9] Shan Gao. "A preemptive priority retrial queue with two classes of customers and general retrial times". In: *Operational Research* 15.2 (Apr. 2015), pp. 233–251. ISSN: 1866-1505. DOI: 10.1007/s12351-015-0175-z.

[10] Sherif I. Ammar and Pakkirisamy Rajadurai. "Performance Analysis of Preemptive Priority Retrial Queueing System with Disaster under Working Breakdown Services". In: *Symmetry* 11.3 (Mar. 2019), p. 419. ISSN: 2073-8994. DOI: 10.3390/sym11030419.

[11] Ruslana Nekrasova. "Stability Conditions of Two-Class Preemptive Priority Retrial System with Constant Retrial Rate". In: *Distributed Computer and Communication Networks*. Springer Nature Switzerland, 2025, pp. 69–80. ISBN: 9783031808531. DOI: 10.1007/978-3-031-80853-1_6.

[12] Konstantin Avrachenkov, Evsey Morozov, and Ruslana Nekrasova. "Stability analysis of two-class retrial systems with constant retrial rates and general service times". In: *Performance Evaluation* 159 (Jan. 2023), p. 102330. ISSN: 0166-5316. DOI: 10.1016/j.peva.2022.102330.

[13] Ruslana Nekrasova et al. "Stability analysis of a two-class system with constant retrial rate and unreliable server". In: *Annals of Operations Research* 331.2 (Feb. 2023), pp. 1029–1051. ISSN: 1572-9338. DOI: 10.1007/s10479-023-05216-6.

[14] Ruslana Nekrasova. "Regeneration estimation in partially stable two class retrial queue". In: *Annales Mathematicae et Informaticae* 56 (2023), pp. 84–94. ISSN: 1787-6117. DOI: 10.33039/ami.2022.12.008.

[15] Evsey Morozov and Bart Steyaert. *Stability Analysis of Regenerative Queueing Models: Mathematical Methods and Applications*. Springer International Publishing, 2021. ISBN: 9783030824389. DOI: 10.1007/978-3-030-82438-9.

[16] G. Fayolle, V. A. Malyshev, and M. V. Menshikov. *Topics in the Constructive Theory of Countable Markov Chains*. Cambridge University Press, May 1995. ISBN: 9780511984020. DOI: 10.1017/cbo9780511984020.